7 Discussion

Our main result is the derivation of the thermal inertia of 5 near-Earth asteroids (NEAs) from analysis of extensive sets of thermal-infrared data using a detailed thermophysical model (TPM). This is the only well-established method to measure the thermal inertia of asteroids, hence it is difficult to gage the reliability of our results in a direct way. Indirect validation comes from studies of the physical consistency of the TPM (see sect. 7.1) and from studies of the consistency and accuracy of TPM-derived diameter estimates (see sect. 7.2). In particular, TPM-derived diameters are found to be in excellent agreement with diameter estimates obtained using other techniques including spacecraft rendezvous, which is a valuable result in its own right. The core section of this chapter is sect. 7.3, in which the thermal inertia of NEAs is discussed in the context of previously available information.

7.1 Thermophysical model (TPM)

Our TPM takes explicit account of the effects of irregular shape, spin pole orientation, surface roughness, and thermal inertia. The model code described in chapter 3 allows for globally convex shapes, generalizations to non-convex shapes are under development (see chapter A in the appendix). As will be discussed in the following, our model has been shown to be applicable to near-Earth asteroids (NEAs) which are more challenging to model than larger objects such as main-belt asteroids (MBAs). We conclude that our TPM is applicable to all asteroids.

7.1.1 Comparison with the Lagerros model

Thermophysical processes are modeled following Lagerros (1996, 1997, 1998a), who proposed the most realistic asteroid TPM currently available (see sect. 3.1). A minor improvement of Lagerros's modeling is proposed in sect. 3.2.3.e on p. 70, where we provide an analytic expression for the multiple scattering of observable thermal flux inside craters to all orders; Lagerros (1998a) only considers direct

emission and single scattering. The effect thereof, however, was found to be negligible for reasonable emissivity values (see Fig. 3.3 on p. 72). Lagerros (1998a) proposed two different ways of modeling thermal conduction inside craters; we have only implemented the numerically more advantageous version, which is potentially less physical (see sect. 3.2.3.f). Lagerros found good agreement between the numerical outcome of both versions for MBA parameters; see sect. 7.1.2 and 7.1.3 for further discussion in the context of NEAs.

The numerical design and implementation of our TPM code is fully independent of Lagerros'. Numerical evaluation of partial differential equations and integrals inevitably involves discretization and truncation, which introduce numerical noise. In the choice of discretization and truncation parameters, the required numerical accuracy must be weighed against the numerical effort. Parameters must be chosen fine enough to guarantee physical output for the purpose at hand, but not too fine in order to avoid excessively long computer run times.

No detailed information on the numerical implementation of Lagerros' model is publicly available. It is clear, however, that numerical efficiency was an important design criterion in the implementation of his model (see Lagerros, 1998b, chapt. 3), which was primarily aimed at application to MBA data. The typical thermal inertia of MBAs is very low, comparable to that of lunar regolith, and ground-based observations of MBAs are restricted to phase angles not largely exceeding 30°. For these circumstances, the Lagerros model is reportedly very accurate and is used, e.g., for the calibration of space telescopes (Müller and Lagerros, 1998, 2002).

Our TPM code, on the other hand, has been designed and tested to be applicable to NEAs, i.e. for a thermal inertia up to that of bare rock (2500 J s$^{-1/2}$K^{-1}m^{-2}) and for very large phase angles, when thermal emission emanating from large portions of the non-illuminated side is observable. We found that a TPM code for NEAs must be designed in a way which is numerically much more expensive than for MBAs (see sect. 7.1.2).

We conclude that our TPM code represents the first detailed TPM shown to be applicable to NEAs. Such a model is required for the determination of their thermal inertia, which is the primary aim of this thesis.

7.1.2 Internal consistency

As a first step, it was carefully verified that the output of the TPM code is internally consistent (see sect. 3.4): Model fluxes were seen to be in agreement with

qualitative expectations (see, e.g., Fig. 3.4 on p. 79 or Fig. 2.2 on p. 29). Furthermore, model fluxes were found to conserve energy provided that sufficiently fine discretization parameters are chosen. In particular, we found the required numerical effort (expressed in terms of a fractional accuracy goal) to increase considerably with increasing thermal inertia. We chose numerical parameters such that model fluxes conserve energy to within a few percent for the thermal inertia of bare rock (2500 J s$^{-1/2}$K^{-1}m^{-2}), better for lower thermal inertia. Our approximate treatment of thermal conduction inside craters (see sect. 3.2.3.f) was found to lead to physically consistent flux values (see sect. 3.4.3).

7.1.3 Consistency with other models

We found TPM-generated synthetic flux values to agree with expectations based on experience with the NEATM (Harris, 1998, see also sect. 2.5). Studies similar to those presented by Delbo' (2004, chapt. 6) have been performed, where TPM-generated synthetic fluxes have been fitted using the NEATM. In those studies, we found that the input diameter was reliably retrieved and that the dependence of the model parameter η on thermal inertia and roughness was as expected, i.e. that increasing thermal inertia increases η while roughness decreases η for low solar phase angle α and increases η for large α.

TPM results from fits to NEA data (see sections 6.1–6.5) were generally found to be consistent with results obtained using simpler models. In the case of (1580) Betulia (see sect. 6.3), the TPM-derived diameter is ~ 25 % larger than its NEATM-derived counterpart, barely consistent at the combined 1σ level; the TPM result has later been supported through radar-derived estimates. In our study of the NEA (33342) 1998 WT24 (see sect. 6.5), TPM-generated fluxes were seen to agree with the output of an independently developed, less detailed TPM. In our study of the NEA (25143) Itokawa (see sect. 6.2), we have, among other things, re-analyzed a data set which had previously been analyzed using Lagerros' model. Good mutual consistency of the results was found implying, in particular, that our approximate treatment of thermal inertia inside craters (see sect. 3.2.3.f) is uncritical at least for a thermal inertia up to 700 J s$^{-1/2}$K^{-1}m^{-2}.

7.1.4 Consistency of results with "ground truth"

Two of the NEAs studied by us, Eros (see sect. 6.1) and Itokawa (see sect. 6.2), have been rendezvoused by spacecraft. In both cases, our TPM-derived diameter

estimates are in excellent agreement with spacecraft results (see sect. 7.2 for a detailed discussion). No independent technique for measuring thermal inertia has been established so far, hence it is more difficult to gage the accuracy of our thermal-inertia results. At least in the case of Eros, however, our results are in excellent agreement with qualitative expectations based on a geological interpretation of the surface makeup, while our results for Itokawa are subject to discussion (see sect. 7.3). In the case of the MBA Lutetia (see sect. 6.6), ground truth will become available after the Rosetta flyby in 2010.

7.1.5 Model applicability

Compared to simpler models, TPMs inevitably contain a larger number of free parameters, such that a larger set of thermal-infrared data is required to constrain the model parameters in a meaningful way. Furthermore, some knowledge on the global shape and spin state is required, which must be obtained using other techniques.

Typically, very little is known about NEA shapes and spin states (see sect. 1.5.4), while thermal-infrared observations are notoriously difficult (see sect. 2.3). Therefore, one has little choice but to use a "simple" thermal model for the analysis of thermal-infrared observations of all but the best studied asteroids. This has imposed significant difficulties on studies of the thermal inertia of NEAs so far.

There is, however, an ever-increasing number of objects with known shape and spin state, including many NEAs; optical telescope systems which are currently being built promise to increase their number by the thousands in the near future (Ďurech et al., 2005). At the same time, progress in infrared detector technology and the sophistication of modern space telescopes including the Spitzer Space Telescope (see chapter 5) render high-quality spectrophotometric or spectroscopic thermal-infrared observations of faint asteroids much more feasible than in the past.

Required data quality We have found that determination of thermal inertia imposes generally more stringent requirements on the data quality than estimation of diameter and albedo. This is nicely exemplified in our analysis of four different sets of thermal-infrared data of (25143) Itokawa (see sect. 6.2), where even the two data sets which did not significantly constrain the thermal inertia allowed the diameter to be determined to within 10 % of the Hayabusa result or better.

Accuracy of thermal-inertia results   The analysis of thermal-infrared observations using a TPM is the only established technique to measure the thermal inertia of individual asteroids. The use of simpler models entails significant systematic uncertainties; see, e.g., previous estimates of the thermal inertia of Itokawa (sect. 6.2) or Betulia (sect. 6.3), which were found to be flawed. While this fact underlines the importance of our studies, it also prohibits methodologically independent cross-checks on our thermal-inertia results. Our diameter and albedo results are in excellent agreement with estimates obtained using other techniques such as spacecraft imaging (see sect. 7.2), inspiring trust into the accuracy of our thermal-inertia results. Note that in the case of (1580) Betulia (see sect. 6.3) our results for diameter and albedo were in contrast with previous estimates dating from the 1970s. However, after the publication of our results (Harris et al., 2005a), our results were independently confirmed based on reanalyses of old data and newly obtained radar observations (Magri et al., 2007).

7.1.6 One-dimensional heat conduction

Our model neglects the effects of lateral heat conduction. This is justified for shape models where the typical linear dimensions of facets are large compared to the thermal skin depth, which ranges between millimeters up to ~ 50 cm depending on the surface material. We would therefore expect our TPM code to be applicable to all shape models with a resolution at the meter scale or coarser, comprising practically all currently available asteroid shape models.[1]

Any realistic shape model for very small objects below some 10 m in diameter must have very small facets, such that our TPM would not be applicable to such small objects. No information on the shape and spin state of such small objects is currently available.

7.2 Accuracy of TPM-derived diameter estimates

The accuracy of TPM-derived diameter estimates for asteroids depends critically on the quality and extensiveness of the available thermal-infrared database and on the quality of the used model of the asteroid shape and spin state. However, the assumptions and approximations made in the thermophysical modeling add

---

[1] An exception may be high-resolution version of the Hayabusa-derived shape model of Itokawa with more than 3 million facets over a body with an effective diameter around 0.32 km, corresponding to an average facet size around 0.1 m^2.

to the error budget. We expect our modeling to be much more realistic than that of "simple" thermal models and would therefore expect considerably smaller systematic modeling uncertainties. The latter may nevertheless be the dominant source of uncertainty if both an extensive set of high-quality data and an accurate shape model are available.

Generally speaking, the requirements for a reasonably accurate determination of the diameter are less stringent than for constraining the thermal inertia (see sect. 7.1.5)—this is the physical basis of the applicability of "simple" thermal models.

NEAs rendezvoused by spacecraft To study the systematic diameter uncertainty inherent in our modeling, we found it instructive to determine the diameter of those two NEAs whose diameter, shape, and spin state have so far been determined very accurately during a spacecraft rendezvous, namely (433) Eros and (25143) Itokawa. We have analyzed thermal-infrared observations of both asteroids (the data were partially obtained by us) using our TPM. Our model neglects the effect of concavities beyond the size scale of single facets (i.e. beaming due to cratering) although major global-scale concavities are present in the shape of both asteroids (see, e.g., Fig. 6.1 on p. 139 and Fig. 1.1 on p. 2). Most thermal-infrared observations of these objects were obtained at moderate solar phase angles around 30°, although our Itokawa database contains 5 data points obtained at 108°. Shadowing effects due to large-scale surface profile would be expected to be more important at larger phase angles, potentially leading to large diameter uncertainties.

Nevertheless, our diameter estimate for Eros is within ~ 5 % of the spacecraft-derived result (see sect. 6.1). Our best estimate of Itokawa's diameter (see sect. 6.2) is within the 2 % uncertainty range of the spacecraft-derived value. While these two studies alone do not allow one to constrain the systematic uncertainty in a statistically significant way, they do show that TPM-derived diameters are potentially very accurate. A fractional diameter uncertainty of 10 % appears to be a conservative upper limit on the systematic uncertainty inherent in our TPM. We speculate that the actual diameter accuracy may be better, but more than two "ground truth" values would be required to confirm this. Upcoming space missions to NEAs (see sect. 1.1) are expected to provide further accurate diameter estimates, which will allow our analysis to be refined.

Large phase angle   One may expect the diameter accuracy to decrease with increasing solar phase angle at which observations have been obtained. Our study of the NEA 1998 WT24 (see sect. 6.5) is reassuring in this respect, where all thermal-infrared data were obtained at phase angles above 60°. Several independent estimates of the object's diameter are available (see table 6.9), all of which are consistent with our result at the 10 % level despite the large phase angle.

Radar   The analysis of radar echoes of asteroids is a well established technique to measure their diameters (see Ostro et al., 2002) that is completely independent of ours. Radar-derived diameters of our targets Itokawa, Betulia, YORP, and Lutetia have been published (see the discussion in sections 6.2, 6.3, 6.4, and 6.6, respectively). In each case, diameter estimates are mutually consistent at the combined 1σ level. However, the nominal radar-derived diameters are consistently ~ 15 % larger than the nominal TPM-derived diameters. It remains to be studied whether or not there is a statistically significant diameter difference. In the case of Itokawa, the Hayabusa result nicely confirms our estimate but is $\sim 1.3\sigma$ below the nominal radar-derived result by Ostro et al. (2005). No such "ground truth" is available for Betulia and YORP; we note that these objects display concavities which are relatively larger than on Itokawa, potentially lowering the accuracy of our results in their case (see sect. 7.3.4.b). In the case of Lutetia, ground truth will become available after the Rosetta flyby in 2010.

Flux calibration   We note that diameter estimates based on thermal observations are in principle susceptible to uncertainties in the absolute flux calibration, which used to plague early thermal-infrared studies. Since the work of, e.g., Cohen et al. (1996, 1999) this uncertainty has been reduced drastically; Reach et al. (2005), e.g., report an uncertainty of 3 % in the absolute flux calibration of the IRAC camera (see sect. 5.2) on board the Spitzer Space Telescope. Since asteroid flux levels scale with the projected area, the corresponding diameter uncertainty is only 1.5 %.

7.3 Thermal inertia of NEAs

From TPM-analyses of extensive sets of thermal-infrared data, we have determined the thermal inertia of 5 NEAs, thus increasing the total number of NEAs with measured thermal inertia to 6. For two of our targets, we refine previously available

Table 7.1: Summary of all thermal-inertia measurements of NEAs currently available. As detailed in sect. 6.1 and 6.2, our thermal-inertia measurements of Eros and Itokawa are expected to supersede earlier determinations by Lebofsky and Rieke (1979) and Müller et al. (2005), respectively (our Itokawa result is partially based on data reported in Müller et al., 2005). Lebofsky and Rieke's estimate of Eros' dimensions was converted by us into a volume-equivalent diameter using eqn. 2.1; the spacecraft-derived value is 16.9 km.

NEA	Diameter (km)	Thermal inertia ($J\,s^{-1/2}K^{-1}m^{-2}$)	Source
(433) Eros	17.8 ± 1.8	150 ± 40	Sect. 6.1
(25143) Itokawa	0.32 ± 0.03	700 ± 100	Sect. 6.2
(1580) Betulia	4.57 ± 0.46	180 ± 50	Sect. 6.3
(54509) YORP	0.092 ± 0.010	200–1200	Sect. 6.4
(33342) 1998 WT24	0.35 ± 0.04	200 ± 100	Sect. 6.5
(433) Eros	(24.8)	140–280	Lebofsky and Rieke (1979)
2002 NY40	0.28 ± 0.03	100–1000	Müller et al. (2004)
(25143) Itokawa	0.32 ± 0.03	750 ± 250	Müller et al. (2005)

estimates, no reliable estimates have been available for the remaining three. The diameter range spanned by our targets is 0.1–17 km (see table 7.1). As will be discussed in the following, our results allow the first firm conclusions to be drawn on the typical thermal inertia of NEAs.

7.3.1 Thermal-inertia results in context

Previously available information   Before the start of the work towards this thesis, the thermal inertia of a single NEA, (433) Eros, had been measured (Lebofsky and Rieke, 1979, see sect. 6.1 for a discussion). In the meantime, two more thermal-inertia measurements of NEAs have been reported (Müller et al., 2004, 2005), based on the Lagerros TPM (see also sect. 7.1.1). Some indirect and consequently unreliable inference on the thermal inertia of NEAs was drawn from results of simple thermal models (see sect. 1.5.8 for an overview). In the cases of (1580) Betulia (see sect. 6.3) and (25143) Itokawa (see sect. 6.2), we found such estimates to be flawed.

From a measurement of the Yarkovsky-induced orbital drift of the NEA (6489) Golevka (effective diameter ~ 0.53 km), Chesley et al. (2003) derive a thermal conductivity around 0.01 W $K^{-1}m^{-1}$ depending on the unknown bulk mass density of the object. They note that values in excess of 0.1 W $K^{-1}m^{-1}$ would also result in a good fit to their data. The corresponding thermal-inertia values are[2]

---

[2] The heat capacity assumed by Chesley et al. (2003) is not stated explicitly, but quoted by

~ 100 J s$^{-1/2}$K^{-1}m^{-2} and > 340 J s$^{-1/2}$K^{-1}m^{-2}. They rejected the latter as "unrealistically high", which appears unjustified in the light of our results (see table 7.1).

Typical thermal inertia of NEAs   The weighted average of the 6 thermal-inertia values reported in table 7.1 (disregarding the superseded previously available estimates for Eros and Itokawa) is 212 J s$^{-1/2}$K^{-1}m^{-2} (weighted by absolute uncertainty) or 400 J s$^{-1/2}$K^{-1}m^{-2} (weighted by fractional uncertainty). We conclude that the typical thermal inertia of NEAs is moderately high, roughly 300 J s$^{-1/2}$K^{-1}m^{-2}, with a significant scatter exceeding a factor of two.

Such values are more than an order of magnitude above typical values for large MBAs (around 15 J s$^{-1/2}$K^{-1}m^{-2}, see Müller and Lagerros, 1998), yet around an order of magnitude below that of bare rock on Earth (see table 3.1 on p. 58). In particular, our results display an apparent trend of increasing thermal inertia with decreasing asteroid size (see sect. 7.3.2). See sect. 7.3.3 for a discussion of implications on the surface structure of NEAs.

Yarkovsky effect   Our thermal-inertia result is of immediate relevance for studies of the important Yarkovsky effect (see sect. 1.3) which is governed by thermal inertia. Our results imply that for model calculations of the Yarkovsky or YORP effects a typical thermal inertia around 300 J s$^{-1/2}$K^{-1}m^{-2} should be assumed, more than an order of magnitude higher than that derived for MBAs. This corresponds to a thermal conductivity of ~ 0.08 W K^{-1}m^{-1} assuming a heat capacity of 680 J kg^{-1}K^{-1} and a near-surface bulk density of 1700 kg m^{-3}.

The implications of our thermal-inertia result on the magnitude of the Yarkovsky effect for individual asteroids depends on other parameters such as the heliocentric distance, orbital eccentricity, and spin axis obliquity; for plausible parameters, the Yarkovsky effect is a strong function of thermal inertia (e.g. Bottke et al., 2006). See Vokrouhlický et al. (2000, Fig. 5) for the thermal-conductivity dependence of the Yarkovsky-induced orbital drift of several NEAs; see Morbidelli and Vokrouhlický (2003, Fig. 5) for an analogous plot for spherical objects in the inner main belt.

Our results are expected to enable a more accurate assessment of the impact hazard posed by individual objects such as (29075) 1950 DA, the object with the

---

Bottke et al. (2006) to be 680 J kg^{-1}K^{-1}. The quoted thermal conductivity corresponds to a near-surface mass density of 1700 kg m^{-3}.

currently highest known Earth impact probability (see sect. 1.4), where the orbital uncertainties are dominated by the lack of knowledge on physical parameters governing the Yarkovsky effect (Giorgini et al., 2002).

Recent confirmation by Delbo' et al. (2007a)   Our result for the typical thermal inertia of NEAs has recently been confirmed in a complementary study by Delbo' et al. (2007a).[3] While herein we determine the thermal inertia of individual NEAs (and are therefore limited to a small number of objects for which information on shape and spin state is available and require extensive sets of thermal-infrared data for each object), Delbo' et al. consider the much larger sample of NEAs with published multi-wavelength thermal-infrared observations. No attempt was made at constraining the thermal inertia of individual objects but rather the ensemble-average thermal inertia was determined. They obtain 200 ± 40 J s$^{-1/2}$K^{-1}m^{-2} for the average thermal inertia of an ensemble of NEAs clustering around 1 km in diameter, in excellent agreement with our average value of 300 J s$^{-1/2}$K^{-1}m^{-2}, keeping the large scatter of roughly a factor of two in mind.

While the lack of knowledge on important physical properties of their individual targets might induce a significant systematic uncertainty in the Delbo' et al. (2007a) result, our result alone may be thought to lack statistical significance, being based on a sample of only 6 NEAs. The excellent mutual consistency of the results of these two complementary thermal-inertia studies greatly supports the validity of both.
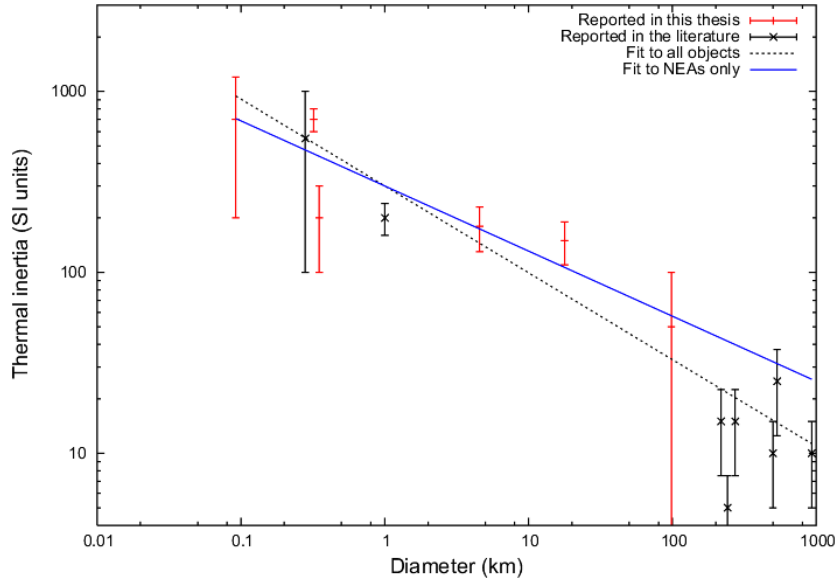
7.3.2 Thermal inertia correlates with size

There is an intriguing correlation between the thermal inertia and diameter of asteroids (see Fig. 7.1). The available thermal-inertia measurements of asteroids are:[4]

- those reported in table 7.1 on p. 222

- the result by Delbo' et al. (2007a) discussed above

- the thermal inertias of (1) Ceres, (2) Pallas, (3) Juno, (4) Vesta, and (532) Herculina reported by Müller and Lagerros (1998)

---

[3] I am a coauthor of that paper.

[4] Our result for the thermal inertia of (617) Patroclus (see sect. 6.8), a Trojan, is disregarded. It is unclear at present whether or not the surface structure of Trojans is comparable to that of inner-Solar-System asteroids.

Figure 7.1: Results of all currently available measurements of the thermal inertia of asteroids. See text for references. Previous results for Eros and Itokawa, which have been superseded in this thesis, are omitted. The dashed black line is the power-law correlation for all asteroids reported by Delbo' et al. (2007a), the solid blue line is its counterpart considering only NEAs.

- the thermal inertia of (65) Cybele reported by Müller and Blommaert (2004)

- the thermal inertia of (21) Lutetia reported in sect. 6.6 of this thesis.

As can be seen in Fig. 7.1, all values appear to scatter around a straight line on a log-log scale, indicating that thermal inertia Γ and diameter D are related through a power law $\Gamma \propto D^{-\xi}$. From an analysis of all results depicted in Fig. 7.1,[5] Delbo' et al. (2007a) determined the exponent ξ to be ~ 0.48 if all data are considered, and $\xi \sim 0.36$ if only NEAs are considered.

As discussed by Delbo' et al., the apparent thermal-inertia dichotomy between large MBAs and small NEAs is partially caused by the difference in heliocentric distance and correspondingly in temperature; as will be discussed in sect. 7.3.4.a, the thermal inertia of regolith would be expected to depend on the temperature T like $T^{3/2}$, leading to a dependence on heliocentric distance r proportional to $r^{-3/4}$. Correcting the available thermal-inertia results for this effect reduces the thermal-inertia contrast somewhat, but does not remove it, yielding a smaller exponent of

---

[5] Except for (54509) YORP (see sect. 6.4), which corresponds to the leftmost data point in Fig. 7.1, and is not yet published. Note the consistency of that point with the extrapolation of the correlation found.

$\xi \sim 0.37$ for the size-dependent thermal inertia of the entire ensemble.

We conclude that there appears to be a significant correlation of thermal inertia with size, although more data would be valuable to confirm the trend.

Size dependence of the Yarkovsky effect If thermal inertia were size independent, the Yarkovsky force would be proportional to D^2. Since the mass scales with D^3, the resulting strength of the Yarkovsky effect is proportional to D^{-1} (see sect. 1.3). The apparent correlation of thermal inertia and size, however, implies a weaker dependence, roughly proportional to $D^{-0.6}$ (see Delbo' et al., 2007a).

Size-frequency distributions of NEAs and MBAs The Yarkovsky effect determines the size-dependent efficiency of the delivery of small asteroids from the main belt into near-Earth space (Morbidelli and Vokrouhlický, 2003, see also sect. 1.2). The size dependence of the Yarkovsky-induced orbital drift should therefore be reflected in a difference in the size-frequency distribution (SFD) of NEAs compared to MBAs in the same size range. In particular, the weaker size dependence of the Yarkovsky effect following from our thermal-inertia results (see above) implies that the SFD of NEAs should be less skewed towards smaller sizes than previously assumed.

While the SFD of MBAs at typical NEA diameters is currently not well known, available observational constraints are in better agreement with the SFD implied by our results than with the steeper SFD for size-independent thermal inertia (see Delbo' et al., 2007a, and references therein).

7.3.3 Geological interpretation

7.3.3.a Is there regolith on NEAs?

We find the typical thermal inertia of NEAs to be intermediate between that of lunar regolith and bare rock on Earth. This suggests that NEAs are covered with particulate materials, where the thermal inertia increases with typical grain size (see sect. 3.2.2.b on p. 56). In particular, the observed size-dependence of thermal inertia is readily explained in terms of regolith coarseness and/or abundance (see also sect. 7.3.3.b).

No convincing evidence has yet been found for very high thermal inertia "bare-rock" surfaces amongst NEAs. Even the $D \sim 100$ m ultra-fast rotator (54509)

YORP appears to have at least some regolith on its surface, despite the large centrifugal force which overwhelms the surface gravity (see also sect. 7.3.3.c).

Relations between grain size and thermal conductivity are well established for the atmospheric conditions prevailing on Earth and Mars, but not for a vacuum. In particular, Presley and Christensen (1997) found that even under the thin Martian atmosphere heat transfer is dominated by atmospheric transfer.[6] Laboratory measurements similar to those reported by Presley and Christensen but obtained in a higher vacuum may be required to correlate the thermal inertia of asteroids with a typical grain size.

Nevertheless, all thermal-inertia values of NEAs measured so far (see table 7.1 on p. 222) are significantly larger than that of lunar regolith, implying that asteroidal regolith is coarser than lunar regolith and/or not much deeper than the thermal skin depth (which is of the cm scale). This agrees nicely with results of spacecraft observations of Eros and Itokawa, which revealed coarser-than-lunar regolith on Eros (see Veverka et al., 2001a,b) and coarser-than-Eros regolith on Itokawa (Yano et al., 2006).

7.3.3.b Size-dependent efficiency of regolith formation

While it is not yet fully understood how regolith on asteroids forms, it is widely believed to be generated during impact processes and to be retained by asteroidal gravity (see sect. 1.5.7). In this picture, one would expect small bodies with low gravity to lose most of their ejecta towards space, and the particle size distribution of the retained ejecta to be skewed towards particles with lower thermal velocity, i.e. towards larger particles relative to the original ejecta distribution. Furthermore, smaller bodies have lower collisional lifetimes, so small NEAs might be disrupted before they have built up a thick layer of regolith depending on the (largely unknown) typical timescale for regolith formation.

It is therefore natural to expect that the regolith on smaller asteroids is less abundant and coarser than on larger asteroids, leading to enhanced thermal inertia. Hence, the existence of a size dependence of thermal inertia does not come as a big surprise as such. However, the form and parameters of this dependence are not constrained by our currently incomplete theoretical understanding. It was actually widely expected that sub-km NEAs should not be able to retain regolith at

---

[6] This is not explicitly stated by Presley and Christensen, but implied by their extrapolation formulae for the thermal conductivity as a function of atmospheric pressure (e.g. their eqn. 17) which yield zero for zero pressure.

all. Our findings imply that Itokawa, which has been demonstrated by Hayabusa imaging to be at least partially covered in regolith, appears to be the rule rather than an exception.

It appears to be well established that physical properties of the asteroid material, chiefly its porosity, greatly influence the amount of produced ejecta, its velocity distribution, and furthermore the size-frequency distribution of ejected particles. Furthermore, a body's ability to gravitationally retain regolith depends not only on its size but also on its bulk mass density.

The size dependence of thermal inertia will serve as a valuable constraint for future modeling of impact processes on asteroids and for the physical properties of asteroids. We speculate that the presence of regolith on small asteroids indicates a large porosity in their near-surface layers, which would be expected to lower ejecta velocities relative to an impact into solid material (see sect. 1.5.7).

Furthermore, one may expect the correlation between size and thermal inertia to differ between members of different taxonomic classes, which appear to display different mineralogy and different bulk mass density. We speculate that this is the reason for the large difference in thermal inertia found between the NEAs Itokawa (S type) and 1998 WT24 (E type), which are roughly equal in size (see table 7.1 on p. 222). However, significantly more data are required to confirm this expectation.

Finding possible taxonomy-dependent differences in thermal inertia might stimulate further progress in the modeling of impact processes, which is of crucial importance for many aspects of planetary research including age determination of planetary surfaces and the assessment of the hazard due to impacts on Earth.

7.3.3.c What is the "bare rock" on NEAs?

All of our NEA targets display a thermal inertia much below that of bare rock on Earth, which is ~ 2500 J s$^{-1/2}$K^{-1}m^{-2} (see, e.g., table 3.1 on p. 58 or Jakosky, 1986). This is rather surprising, in particular for (54509) YORP and (25143) Itokawa, which one may expect to display a larger thermal inertia than actually found.

(54509) YORP   YORP is an ultrafast rotator with a diameter of only ~ 0.1 km (see sect. 6.4). Its fast spin rate of ~ 12 min implies that the centrifugal force overwhelms gravity on most of its surface, hence dust cannot be retained by gravity except for small parts of the surface close to the rotational poles. Nevertheless,

our preliminary result for its thermal inertia is only 200–1200 J s$^{-1/2}$K^{-1}m^{-2}, much below that of bare rock but consistent with the size dependence obtained from our remaining results (see Fig. 7.1 on p. 225, note that the best-fit straight line therein was derived by Delbo' et al., 2007a, *without* our YORP result), which we interpret in terms of regolith coarseness and/or abundance (see above). We caution, however, that our result for YORP is preliminary (see sect. 6.4.4).

(25143) Itokawa We found Itokawa, the target of the Japanese rendezvous mission Hayabusa, to have a thermal inertia of 700 $\pm$ 100 J s$^{-1/2}$K^{-1}m^{-2}, refining the estimate by Müller et al. (2005, 750 $\pm$ 250 J s$^{-1/2}$K^{-1}m^{-2}, see sect. 6.2). However, Hayabusa imaging clearly demonstrates that $\sim$ 80 % of the surface are dominated by boulders and only $\sim$ 20 % are covered in coarse regolith.

Tentative interpretation in terms of a thin dust coating We speculate that boulders on Itokawa are (partially?) covered with a thin layer of thermally insulating material such as dust, potentially through cohesion. Such a coating would significantly reduce the thermal inertia provided its thickness is a non-negligible fraction of its thermal skin depth ($\sim$ 5 mm for fine dust on Itokawa). To the best of our knowledge, such a dust coating is neither indicated nor ruled out by Hayabusa imaging results published so far. All Hayabusa data have recently (24 April 2007) been made publicly available; we hope they will shed light on the issue at hand. Cohesion between regolith particles has frequently been discussed in the context of NEAs (e.g. Cheng, 2004b; Colwell et al., 2005; Starukhina, 2005); cohesive attraction appears to be stronger than gravitational attraction for typical NEAs but depends critically on the (largely unknown) particle size. Fine dust is more cohesive than coarse dust. This may explain why fine dust apparently sticks to boulders, despite the fact that coarser pebble-sized grains were found to be mobile by Miyamoto et al. (2007).

On YORP, dust is destabilized by the centrifugal force, which overwhelms gravity. It can be shown, however, that the former is only of the order of 10^{-3} m s^{-2}, the latter is still smaller. In the light of the above, it appears plausible that cohesion can stabilize fine dust on the surface of YORP. We also note that, due to the fast spin rate, the thermal skin depth is much lower than on other objects (smaller by a factor of $\sim \sqrt{120} \sim 11$ compared to the skin depths for spin period of 24 h quoted in table 3.1 on p. 58), hence a dust "thickness" of a fraction of a millimeter is sufficient to reduce the thermal inertia appreciably.

Alternative interpretation in terms of porosity Müller et al. (2005) speculate that the thermal inertia of Itokawa may indicate porous rock (see also sect. 6.2.4 on p. 151). This conforms with the fact that NEAs appear to be typically under-dense. They are thus assumed to contain major voids (see sect. 1.5.5), although virtually nothing is known about the size scale of those voids. If the lower-than-expected thermal inertia of Itokawa and YORP is indeed due to porosity of boulders exposed at the surface, this would imply that near-surface pores are small compared to the thermal skin depth for bare rock (i.e. up to a few cm—see table 3.1 on p. 58). Such information would be relevant for impact modeling. However, it seems to us that an unrealistically large porosity would be required to reduce the thermal inertia by a factor of 2500/700.

7.3.3.d Comparison with Martian satellites

It is instructive to compare our asteroid thermal-inertia results with thermal-inertia values derived for the Martian satellites, Deimos and Phobos, which are spectroscopically similar to asteroids (e.g. Rivkin et al., 2002) and are widely believed to be captured asteroids. Deimos and Phobos bracket Eros in size and are intermediate between NEAs and MBAs in terms of heliocentric distance.

From Viking observations, Deimos and Phobos are known to be covered with regolith; Lunine et al. (1982) report thermal-inertia measurements resulting in 25–84 J $s^{-1/2}K^{-1}m^{-2}$ for Deimos ($D \sim 12.6$ km) and 38–67 J $s^{-1/2}K^{-1}m^{-2}$ for Phobos ($D \sim 22.4$ km). The latter is consistent with the independent thermal-inertia estimate of 20–40 J $s^{-1/2}K^{-1}m^{-2}$ by Kührt et al. (1992) based on infrared observations of Phobos obtained with the Soviet Phobos-2 spacecraft.

To facilitate comparison of these values (obtained at a heliocentric distance of ~ 1.5 AU) with values obtained in the hotter thermal environment of near-Earth space, they must be multiplied by $1.5^{3/4} \sim 1.4$, resulting in 35–118 J $s^{-1/2}K^{-1}m^{-2}$ for Deimos and 28–94 J $s^{-1/2}K^{-1}m^{-2}$ for Phobos. While these values may be larger than the lunar value, they are somewhat below the thermal inertia of Eros and significantly below that of smaller NEAs.

We conclude that the Martian satellites appear to have a finer regolith than asteroids in their size range (e.g. Eros), possibly as fine as lunar regolith. In their case, regolith formation may be aided by the gravitational influence of Mars, which would be expected to influence the ejecta dynamics appreciably. Additionally, impacts on Mars produce fine ejecta which may be captured by its satellites; this is supported by recent Mars Express results obtained with the High Resolution

Stereo Camera HRSC, which indicate that Phobos captured groove-forming Martian ejecta (Murray et al., 2006). Phobos continues to be observed with HRSC (Oberst et al., 2006).

Another possibility to explain the difference in thermal inertia between Eros and the Martian satellites is their different composition: Eros is a silicaceous S-type asteroid, while D or T-type asteroids provide the closest spectral match to the Martian satellites (Rivkin et al., 2002). Our sample of NEA targets does not contain D or T-type asteroids, but a member of the spectrally similar C class, (1580) Betulia. Betulia, with a diameter of $\sim 40\,\%$ of Deimos', has a thermal inertia of $180 \pm 50\ \mathrm{J\,s^{-1/2}K^{-1}m^{-2}}$, significantly above that of the Martian satellites.

7.3.4 Possible improvements to the TPM

7.3.4.a Non-homogeneous thermal properties

In our TPM, all thermal properties are assumed to be homogeneous over the asteroid surface. Furthermore, it is assumed that they do not vary with depth nor temperature. It may be instructive to relax some of these modeling assumptions.

Thermal inertia variegation   As discussed in sections 6.2 and 7.3.3.c, Itokawa displays a dichotomy between rocky "rough" and regolith-dominated "smooth" terrains, although it is not clear whether the boulders in the rough terrain are "bare" or covered with a thin coating of dust. Exposed boulders would display a dramatic contrast in thermal inertia relative to regolith, while already a thin dust coating would reduce the contrast appreciably.

This may be studied using a generalized TPM, in which the surface is decomposed into disjoint units with constant thermal inertia over each unit but possible differences in thermal inertia from unit to unit. A natural choice of such units on Itokawa's surface would be the smooth and rough terrains, which are reportedly well distinguishable on the shape model by Demura et al. (2006).

In the case of Itokawa, the dichotomy between smooth and rough terrains is caused by mobility of regolith, which concentrates in the minima of the combined gravitational-centrifugal potential (Fujiwara et al., 2006; Miyamoto et al., 2007). This may be expected to be generic to small NEAs. It is possible to determine the gravitational-centrifugal potential of other NEAs if a detailed shape model is available; e.g. the paper describing Betulia's radar-derived shape (Magri et al., 2007) contains an extensive discussion of local minima and maxima of the

potential. The study of such objects may benefit from a generalized TPM which allows variegation of thermal inertia. Note that, while the total number of small NEAs well-studied at radar or thermal-infrared wavelengths is small compared to the total number of NEAs, these two samples overlap strongly since they are essentially drawn from the much smaller sample of NEAs which made very close approaches with the Earth within the past few years.

A further application of thermal-inertia variegation may be generalized models of roughness at a small scale, e.g. by means of craters as in our present TPM. It may prove fruitful to assign different thermal-inertia values to facets of different slopes, with a natural first choice being to distinguish between facets with slopes above and below reasonable estimates for the angle of friction of regolith.

Two-layer model In order to test our hypothesis of a thin dust coating on YORP and on the exposed boulders on Itokawa (see sect. 7.3.3.c), a TPM should be developed in which two horizontal layers of different thermal inertia are considered. Similar models have been used before, e.g. to analyze eclipse observations of the Galilean satellites (Morrison and Cruikshank, 1973) or for model calculations of the Yarkovsky effect (e.g. Vokrouhlický and Brož, 1999).

While we caution that such a model is probably poorly constrained in practical application to thermal-infrared data, we expect it to be useful for theoretical studies. In such studies, our current TPM would be used to fit synthetic flux values generated for bare rock covered with dust coatings of different thickness. The resulting effective thermal inertia as a function of dust thickness would aid the interpretation of thermal inertia results.

Temperature dependence In principle, all thermal properties, such as thermal conduction, heat capacity, and also surface bulk density, vary with temperature T, leading to a temperature dependence of the thermal inertia, which is neglected in our model. Temperature dependence of thermal inertia would be expected to influence diurnal surface-temperature distributions directly, but also indirectly through its influence on the sub-surface temperature profile.

While one may expect the heat capacity and bulk density to be negligibly weak functions of T for the conditions relevant to our purposes,[7] the thermal conduction

---

[7] Ghosh and McSween (1999) discuss the temperature dependence of the heat capacity. Their findings (see their Fig. 1) imply that for temperatures of 300–400 K the heat capacity is constant to within 10 % or better for plausible asteroid materials, inducing thermal-inertia variability of 5 % at most ($\Gamma \propto \sqrt{\kappa}$).

may vary greatly with T depending on the heat transfer mechanism (see also the discussion in sect. 3.2.2.b). Purely radiative heat transfer, in particular, is characterized by a thermal conductivity proportional to T^3, implying a thermal inertia proportional to $T^{3/2}$. Purely conductive heat transfer, on the other hand, leads to a virtually constant thermal conductivity. From Apollo-era studies it is well known that both heat-transfer mechanisms are relevant in the lunar regolith (while the third basic heat transfer mechanism, convection, is clearly irrelevant on atmosphereless bodies).

The relatively large thermal-inertia values found by us on NEA surfaces argue in favor of a conduction-dominated heat transfer, and therefore appear to justify our modeling assumption of temperature-independent thermal inertia in hindsight. It would be instructive, nevertheless, to double-check our results using a model with, e.g., T^3 thermal conductivity or a mixed model, where thermal conductivity is a sum of a constant term and a T^3 term. We caution that the thermal-infrared data typically available for NEAs would be expected to be insufficient to constrain an additional fit parameter, such as the relative importance of the two heat transfer mechanisms at a given temperature. Furthermore, to enable meaningful comparison of results obtained from TPMs with different temperature-dependence of thermal inertia, a suitable reference temperature must be defined.

7.3.4.b Non-convex-shape TPM for NEAs

Our thermal-inertia results for NEAs are based on the TPM described in chapter 3, in which the asteroid shape is considered to be convex and neither shadowing nor mutual heating are considered outside craters. If large-scale concavities are present, neglecting them may cause the model temperature distribution to deviate severely from the physical temperature distribution, and may lead to flawed estimates of diameter and thermal inertia. Note that most available asteroid shape models are convex; in particular, shape models derived from the inversion of optical photometry are convex by design (see sect. 1.5.4).

As discussed in sect. 7.2, our diameter results for (433) Eros and (25143) Itokawa are in excellent agreement with spacecraft results despite several prominent concavities on their surfaces. However, in the cases of (1580) Betulia and (54509) YORP our diameter estimates are somewhat below radar-derived estimates, barely within the combined range of uncertainty. While we caution that the reason for this, if any, may also be on the radar side (see sect. 7.2), we note that our observations took place at large solar phase angles of 53° (Betulia) and 59° (YORP). The

radar-derived shape models of both Betulia and YORP display extremely large concavities, with the major concavity on Betulia having a diameter comparable to the asteroid's radius. The difference in nominal diameter estimates is therefore consistent with the expectation that neglecting shadowing effects at large phase angles leads to an underestimation of diameter. Furthermore, we appear to have observed features in the thermal lightcurve which are not well reproduced by our convex-shape TPM (see sect. 6.3.4 and sect. 6.4.4).

It seems worthwhile first to study the available data using a non-convex-shape TPM, in which shadowing is considered but mutual heating is not, before developing a more general TPM, in which mutual heating among facets is considered.

7.3.4.c Brute-force modeling of positive relief such as boulders

As is common practice, we model thermal-infrared beaming by adding synthetic "craters" to the asteroid surface, i.e. indentations which take the shape of sections of hemispheres (see sect. 3.2.3). One may expect this to be a fair approximation for the surfaces of our Moon, Mercury, or other large atmosphereless bodies which are well known to be densely covered with impact craters, which typically have the shape of subdued hemispheres. However, very little is currently known about asteroid surfaces due to the scarcity of available high-resolution spacecraft imaging data. Itokawa, the only sub-km asteroid to be scrutinized by spacecraft so far, was found to be virtually devoid of craters (Saito et al., 2006, see also the discussion in sect. 6.2.4) but most of its surface is dominated by boulders.

Generally, one might expect the thermal effect of positive relief features to be quite different from that of indentations, particularly for observations at large phase angles, when shadowing effects are relatively more important. Thermophysical models with positive rather than negative surface relief have, however, only rarely been considered in the literature (see Lagerros, 1998a, and references therein for a rarely used exception using random surfaces). In particular, no model is known to us in which boulders are specifically considered.

It appears to be worthwhile to develop and study a generalized TPM for NEAs in which roughness is modeled by adding boulders to the surface rather than craters. Suitable geometric boulder models may be hemispherical bulges (if this enables analytical calculations similar to those presented in sect. 3.2.3) or, alternatively, cuboids which would be advantageous for the numerical implementation. Such a study could be based on a general TPM for non-convex shapes which includes the effects of mutual shadowing and heating (see the discussion above).

The main task remaining to be solved would then be to computer-generate very detailed "shape models," where a suitable distribution of boulders is explicitly placed on the surface of a pre-existing shape model. This approach causes the number of surface facets, with which the numerical effort scales, to increase significantly. On the other hand, one thus avoids the computationally very expensive calculation of "crater" fluxes. It remains to be studied whether or not such a "brute-force" modeling of boulders is feasible with currently available computers, possibly after optimizing the TPM code for numerical efficiency.

A test case for such modeling would be to use the shape models of Eros and Itokawa with the highest resolution available, which have 200,700 facets in the case of Eros, and 3,145,728 facets in the case of Itokawa.

7 Discussion